

Purdue University Purdue e-Pubs

Department of Electrical and Computer
Engineering Faculty Publications

Department of Electrical and Computer
Engineering

1990

Orientation-dependent perimeter recombination in GaAs diodes

T. B. Stellwag
Purdue University

Michael R. Melloch
Purdue University, melloch@purdue.edu

Mark S. Lundstrom
Purdue University, lundstro@purdue.edu

M. S. Carpenter
Purdue University

R. F. Pierret
Purdue University

Follow this and additional works at: <https://docs.lib.purdue.edu/ecepubs>

 Part of the [Electrical and Computer Engineering Commons](#)

Stellwag, T. B.; Melloch, Michael R.; Lundstrom, Mark S.; Carpenter, M. S.; and Pierret, R. F., "Orientation-dependent perimeter recombination in GaAs diodes" (1990). *Department of Electrical and Computer Engineering Faculty Publications*. Paper 87.
<http://dx.doi.org/10.1063/1.103108>

This document has been made available through Purdue e-Pubs, a service of the Purdue University Libraries. Please contact epubs@purdue.edu for additional information.

Orientation-dependent perimeter recombination in GaAs diodes

T. B. Stellwag, M. R. Melloch, M. S. Lundstrom, M. S. Carpenter, and R. F. Pierret

Citation: **56**, (1990); doi: 10.1063/1.103108

View online: <http://dx.doi.org/10.1063/1.103108>

View Table of Contents: <http://aip.scitation.org/toc/apl/56/17>

Published by the [American Institute of Physics](#)

Orientation-dependent perimeter recombination in GaAs diodes

T. B. Stellwag, M. R. Melloch, M. S. Lundstrom, M. S. Carpenter, and R. F. Pierret
School of Electrical Engineering, Purdue University, West Lafayette, Indiana 47907

(Received 6 October 1989; accepted for publication 9 February 1990)

Perimeter recombination currents affect the performance of GaAs-based devices such as solar cells, heterojunction bipolar transistors, and injection lasers. We report that the $n \cong 2$ perimeter recombination current has a strong orientation dependence. More than a factor of five variation in the surface recombination current at mesa-etched edges has been observed. These results suggest that with proper device design, perimeter recombination currents could be substantially reduced.

The performance of GaAs-based bipolar devices such as solar cells, heterojunction bipolar transistors (HBTs), and injection lasers can be significantly influenced by the mesa-etched edges which define the device geometry. The current of a mesa-isolated GaAs pn junction is comprised of components due to diffusion of carriers in the bulk neutral regions, recombination in the bulk space-charge region, and recombination at the perimeter of the mesa. Therefore, the current-voltage characteristic of a GaAs pn junction is expected to have the form

$$I = I_{01} (e^{qV/kT} - 1) + J_{0nB} A (e^{qV/nkT} - 1) + J'_{0nP} P (e^{qV/nkT} - 1), \quad (1)$$

where I_{01} is the diffusion saturation current coefficient (A), J_{0nB} is the bulk recombination coefficient (A/cm²), J'_{0nP} is the perimeter recombination coefficient (A/cm), A is the area of the diode, and P is its perimeter. The ideality factors for the bulk and the perimeter components are assumed to be equal. The diffusion saturation current I_{01} has components due to recombination in the bulk neutral regions and at the mesa-isolated edges of the bulk neutral regions. In this work we will focus on the $n \cong 2$ recombination current components.

Henry *et al.*¹⁻⁴ found that the $n \cong 2$ recombination current was dominated by recombination at the exposed perimeter of the mesa for double-heterostructure AlGaAs pn junctions with composition and doping levels similar to those used in injection lasers. The largest device of Henry *et al.*^{2,3} was 125 $\mu\text{m} \times 500 \mu\text{m}$. However, De Moulin *et al.*⁵ have shown that in high-efficiency GaAs solar cells as large as 2 cm \times 2 cm, the $n \cong 2$ recombination current is primarily due to edge recombination. The influence of edge recombination on HBT performance was demonstrated by Sandroff *et al.*⁶ By passivating the periphery with sodium sulfide, Sandroff *et al.* observed a 60-fold increase in the current gain.

We have discovered a strong orientation dependence of the edge recombination current in GaAs pn junctions. In this letter we describe preliminary experiments demonstrating this effect. These results suggest that with proper device design, perimeter recombination currents could be substantially reduced.

The p^+/n diodes of Fig. 1 were designed to suppress the $n = 1$ diffusion current so that the $n \cong 2$ recombination currents could be more easily studied. For long lifetime materials, high surface recombination velocities contribute to a

large $n = 1$ current component. Surrounding the GaAs p^+/n junction with the wider band gap, lattice-matched material $\text{Al}_x\text{Ga}_{1-x}\text{As}$ creates a potential barrier which confines the carriers to the junction region. Since the $\text{Al}_x\text{Ga}_{1-x}\text{As}$ is lattice matched to GaAs, the interface is free of electronic states and therefore has a low surface recombination velocity. Therefore, if the diffusion length is longer than the depth of the region, the $n = 1$ current component is substantially reduced.

The structure of Fig. 1 was grown in a Varian GEN II molecular beam epitaxy (MBE) system. (This MBE system produces very long bulk lifetime material as demonstrated by recent record efficiency MBE-grown GaAs pn heteroface solar cells with structures similar to Fig. 1.⁷) A 2 in. liquid-encapsulated Czochralski (100) GaAs substrate was used. The layers were grown at a substrate temperature of 600 °C. Two gallium furnaces were used with each producing a flux corresponding to a growth rate of 0.5 $\mu\text{m}/\text{h}$. The As_4 to total Ga beam equivalent pressures was 27 as measured with an ion gauge in the substrate growth position. The superlattice (SL) layer consisted of 20 periods of 28 Å $\text{Al}_{0.33}\text{Ga}_{0.67}\text{As}$ barriers and 31 Å GaAs wells. (The SL was incorporated in the film structure to reduce diffusion of impurities from the substrate into the growing film.⁸)

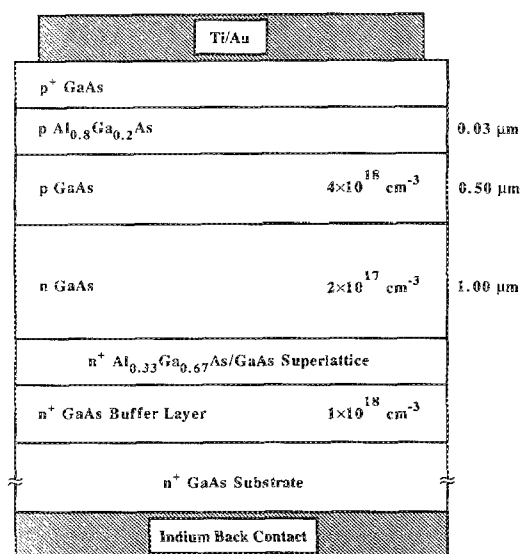


FIG. 1. Cross section of MBE-grown diodes.

Since a nonindium wafer mount was used during the MBE growth, a back ohmic contact was formed by alloying indium at 350 °C for 1 min. Front metallization lift-off patterns were defined, Ti/Au was electron beam evaporated to form nonalloyed ohmic contacts, and the photoresist was dissolved in acetone to remove excess metal. Mesas were defined using conventional photolithography and etched in a 25 °C methanol:H₂O₂:H₂O:H₃PO₄ 3:1:1:1 solution for 1 min, 15 s. The etch rate was approximately 2 μm/min, making this a suitable etch for mesa isolation. [Recently demonstrated record efficiency MBE and metalorganic chemical vapor deposition (MOCVD) grown solar cells have also utilized this mesa isolation etch.^{7,9}]

The finished devices consisted of rectangular diodes where the length of one side was held constant and the other length was varied in order to achieve perimeter to area (P/A) ratios varying from 60 to 440. To study the effects of orientation on the perimeter recombination current, this set of mesa-isolated diodes was rotated at 45° increments on the mask, with subsets rotated at 15° increments. A diode of length a from the set that was rotated every 45° is displayed in Fig. 2. We define 0° as the diode orientation where the side of length a is along the $\langle 011 \rangle$ direction, with the angle of orientation increasing as the diodes are rotated clockwise. Also displayed in Fig. 2 are the mesa-etched profiles observed at 45° increments. The orientation dependence of the mesa-etched profiles shown in Fig. 2 is similar to those previously observed for GaAs.¹⁰

A typical dark current and diode ideality factor as a function of voltage is displayed in Fig. 3. At lower voltages, the measured current of all the diodes has an ideality factor of $n = 1.9$. (The ideality factor varies from $n = 1.9$ to $n = 2.0$ depending on the processing run.) For ease of presentation, this current component is referred to as an $n \approx 2$ recombination current. At higher current levels the ideality factor starts falling as the $n = 1$ diffusion current becomes significant. When series resistance effects become appreciable, a roll-off is observed in the current and a corresponding increase is seen in the ideality factor.

The dark current versus voltage characteristics were measured as a function of device orientation and normalized to 25 °C by accounting for the theoretical change in n_i .¹¹ Shown in Fig. 4 is the recombination saturation current den-

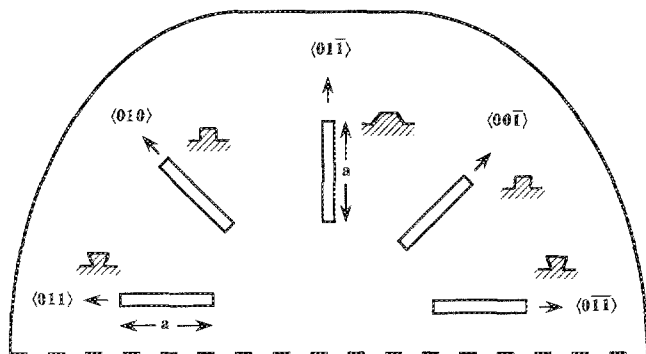


FIG. 2. Mesa-etched profiles as a function of device orientation. The wafer face is a $\langle 100 \rangle$ plane with a $\langle 01\bar{1} \rangle$ wafer flat.

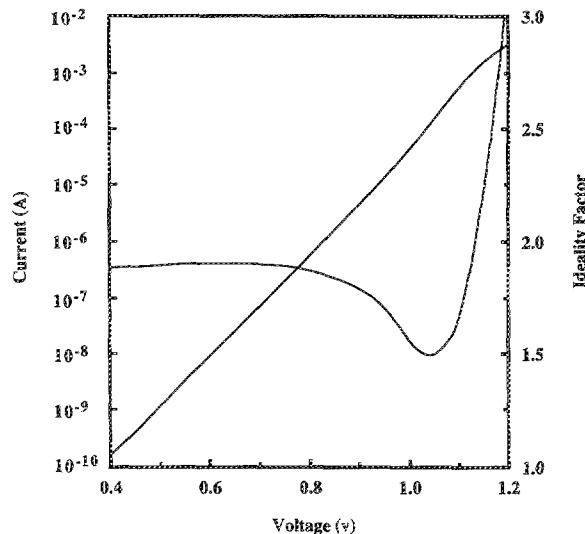


FIG. 3. Typical dark current and diode ideality factor as a function of voltage.

sity (J_{on}) versus the angle of orientation for $70 \mu\text{m} \times 500 \mu\text{m}$ rectangular diodes. Orientation does not affect the bulk component of the $n \approx 2$ current, thus any variation in the current is due to recombination at the perimeter. Since the $n \approx 2$ perimeter recombination current is proportional to the length of the periphery, the majority of the surface recombination occurs along the $500 \mu\text{m}$ side. Figure 4 clearly shows that as the orientation of this dominant side is moved away from the $\langle 011 \rangle$ direction, the $n \approx 2$ recombination current sharply decreases. This shows the strong dependence on device orientation.

Equation (1) assumed a constant J'_{onP} independent of orientation. For a rectangular diode of side lengths a and b , a more accurate description of the current-voltage characteristic of a mesa-isolated GaAs pn junction is therefore

$$I = I_{01} (e^{qV/kT} - 1) + [J_{0nBA} + J'_{0na} 2a + J'_{0nb} 2b] (e^{qV/nkT} - 1), \quad (2)$$

where J'_{0na} is the perimeter coefficient along the sides of

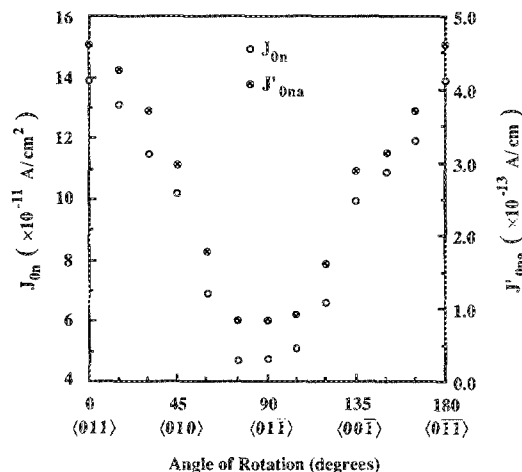


FIG. 4. J_{on} and J'_{0na} as a function of diode orientation at a temperature of 25 °C.

length a and J'_{0nb} is the perimeter coefficient along the sides of length b in A/cm. From Eq. (2) we can write the $n \cong 2$ recombination saturation current density as

$$I_{0n}/A = [J_{0nB} + (2/a)(J'_{0nb} - J'_{0na})] + J'_{0na}P/A. \quad (3)$$

By plotting I_{0n}/A vs P/A ratio for a series of diodes where a is held constant but b is allowed to vary, the perimeter coefficient along the side of length a , J'_{0na} , can be determined from the slope of the plot. As shown in Fig. 4, J'_{0na} varies by more than a factor of 5 with angle of orientation, whereas J_{0n} only varied by a factor of 3. Since the contribution of the recombination current due to the edges aligned at right angles to those of interest is removed, this greater variation in J'_{0na} is expected. Therefore, this extracted value of recombination current gives a truer measure of the orientation dependence.

In Fig. 5, plots of I_{0n}/A vs P/A are shown for sets of diodes at 0° , 45° , 90° , and 135° . The slopes for 45° and 135° show that J'_{0na} is the same for edges along the $\langle 010 \rangle$ or $\langle 001 \rangle$ directions whereas the slopes for 0° and 90° exhibit more than a factor of five difference in J'_{0na} between the $\langle 011 \rangle$ direction and the $\langle 0\bar{1}\bar{1} \rangle$ direction. Once the $n \cong 2$ perimeter recombination coefficients of right angle edges are determined from the slopes of the plot of I_{0n}/A vs P/A , the $n \cong 2$ bulk recombination coefficient can be determined from the intercept of the plot. The value of the $n \cong 2$ bulk recombination coefficient for our diodes is 5.4×10^{-12} A/cm² and the average value of the $n \cong 2$ perimeter recombination coefficient is 2.98×10^{-13} A/cm.

From Fig. 2 it can be noted that the variation in $n \cong 2$ perimeter recombination currents could be attributed to the different mesa-etched profiles. The orientation with the lowest surface recombination corresponds to an outward sloping profile, while the highest corresponds to an undercut profile.

Following Henry and Logan,⁴ the perimeter recombination coefficient J'_{0na} can be written as

$$J'_{0na} = qn_i S_0 L_s, \quad (4)$$

where n_i is the intrinsic carrier concentration, S_0 is the surface recombination velocity, and L_s is an effective surface diffusion length. We find that the $S_0 L_s$ product ranges from 1.49 cm²/s at 0° to 0.27 cm²/s at 90° . The orientation dependence of the perimeter recombination current has important implications for diagnostic structures. Devices with different orientations or different shapes (square, rectangular, circular, etc.) could lead to different conclusions unless the orientation dependence of the $S_0 L_s$ product is taken into account.

In summary, we have experimentally observed that the recombination current at the exposed edges of a GaAs pn

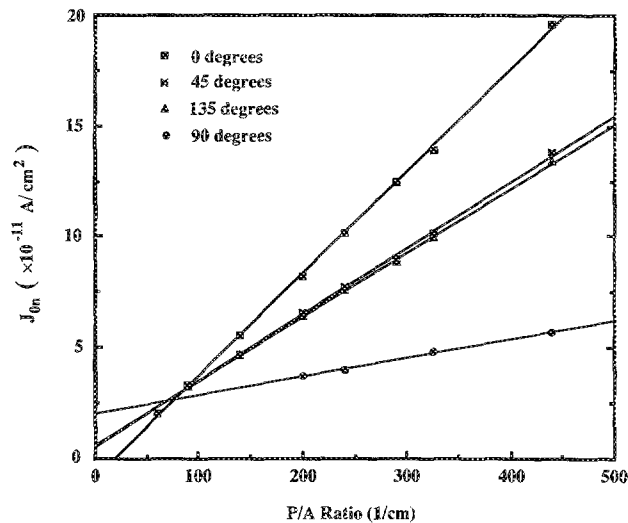


FIG. 5. Plot of extracted I_{0n}/A vs perimeter-to-area ratio for a series of diodes where the side of length a is held constant while the side of length b is varied. The temperature is 25°C and 0° signifies diodes where side a is along the $\langle 011 \rangle$ direction while 90° signifies diodes where side a is along the $\langle 0\bar{1}\bar{1} \rangle$ direction. 45° signifies diodes where side a is along the $\langle 010 \rangle$ direction while 135° signifies diodes where side a is along the $\langle 00\bar{1} \rangle$ direction.

junction has a strong orientation dependence. Variation in the $S_0 L_s$ product at mesa-etched edges by more than a factor of 5 has been measured. These results suggest that with proper device design, perimeter recombination currents could be substantially reduced. It is also important to take the orientation dependence into account when analyzing devices.

This work was supported by the Solar Energy Research Institute for the U.S. Department of Energy under subcontract XL-5-05018-1.

¹C. H. Henry and R. A. Logan, J. Appl. Phys. **48**, 3962 (1977).

²C. H. Henry, R. A. Logan, and F. R. Merritt, Appl. Phys. Lett. **31**, 454 (1977).

³C. H. Henry, R. A. Logan, and F. R. Merritt, J. Appl. Phys. **49**, 3530 (1978).

⁴C. H. Henry and R. A. Logan, J. Vac. Sci. Technol. **15**, 1471 (1978).

⁵Paul D. DeMoulin, Stephen P. Tobin, Mark S. Lundstrom, M. S. Carpenter, and Michael R. Melloch, IEEE Electron Device Lett. **9**, 368 (1988).

⁶C. J. Sandroff, R. N. Nottenburg, J.-C. Bischoff, and R. Bhat, Appl. Phys. Lett. **51**, 33 (1987).

⁷M. R. Melloch, S. P. Tobin, T. B. Steliwag, C. Bajgar, A. Keshavarzi, M. S. Lundstrom, and K. Emery, J. Vac. Sci. Technol. B **8**, 379 (1990).

⁸K. L. Tan, M. S. Lundstrom, and M. R. Melloch, Appl. Phys. Lett. **48**, 428 (1986).

⁹S. P. Tobin, S. M. Vernon, C. Bajgar, S. J. Wojtczuk, M. R. Melloch, A. Keshavarzi, T. B. Steliwag, S. Venkatesan, M. S. Lundstrom, and K. A. Emery, IEEE Trans. Electron Devices **37**, 467 (1990).

¹⁰S. Iida and K. Ito, J. Electrochem. Soc. **119**, 768 (1971).

¹¹J. S. Blakemore, J. Appl. Phys. **53**, 123 (1982).